

Local vibrational modes and compensation effects in Mg-doped GaN

A. Hoffmann*, A. Kaschner, and C. Thomsen

Institut für Festkörperphysik, TU Berlin, Hardenbergstr. 36, 10623 Berlin, Germany

Received 4 March 2003, revised 9 April 2003, accepted 11 April 2003

Published online 28 August 2003

PACS 63.20.Pw, 71.55.Eq, 78.20.-e, 78.30.Fs

The compensation and self-compensation effects in Mg-doped GaN is studied by low-temperature photoluminescence and Raman spectroscopy using a series of samples with different Mg concentrations. Strongly doped samples are found to be highly compensated in electrical measurement. The compensation mechanism is directly related to the incorporation of Mg leading to the additional formation of three different deep donor levels. Furthermore, hydrogen forms defect complexes with Mg and compensates the acceptor states. These complexes were observed as local vibrational modes in Raman spectra in the range of 2200 cm^{-1} . The direct incorporation of Mg can be controlled by local vibrational modes in the region of GaN host phonons. Investigating the intensity dependence of the different Mg–H complexes and the LVM of activated Mg the Raman spectra give a clear direct evidence of the degree of compensation and p-conductivity.

© 2003 WILEY-VCH Verlag GmbH & Co. KGaA, Weinheim

1 Introduction

One of the major advances in semiconductor technology during the recent years was the realization of p-conductivity in GaN leading to optoelectronic devices in the blue spectral range like high-power light-emitting diodes and laser diodes. The major problem to be solved was the compensation of the incorporated Mg-acceptors which resulted in highly resistive material, even at high dopant concentrations. After the breakthrough by Amano et al. [1] using a low-energy electron beam treatment of their p-doped samples Nakamura et al. [2] showed that hydrogen plays an active role in the compensation process. This problem is very similar to the p-doping in II–VI-compound semiconductors with large band gap, like e.g. ZnSe:N [3].

The incorporation of hydrogen is not the only process which leads to a compensation effect. It was found in Mg-doped GaN epilayers that the hole concentration at room temperature is considerable lower than the Mg concentration. The hole concentration as function of the Mg-content in Fig. 1 does not increase continuously, because above a Mg concentration of around 10^{19} cm^{-3} a decrease can be observed [4]. This behavior gives a clear evidence of a strong self-compensation effect. Little is known on the electronic structure of compensating defects and the effects on the optical properties of GaN. We therefore investigated a series of p- and n-type GaN samples with systematically varied concentrations of Mg to gain further insight into the electronically and optical implications of compensation in GaN.

* Corresponding author: e-mail: hoffmann@physik.tu-berlin.de, Phone: +49 30 314 22001, Fax: +49 30 314 22064

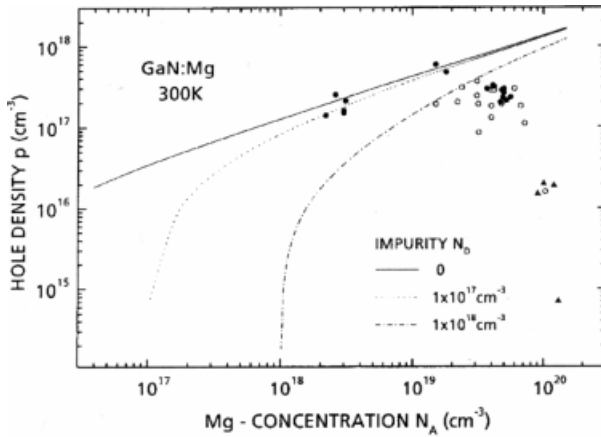


Fig. 1 Hole density in GaN:Mg determined by Hall-measurement at RT as a function of the Mg concentration after [4].

2 Self-compensation effects in GaN:Mg

To examine the self-compensation effects in GaN:Mg a series of samples grown by MOCVD was investigated. The Mg content increases with the Mg/Ga precursor ratio. The samples were annealed at 650°C in a N₂-atmosphere to passivate the H-donors. Below a precursor ratio of 0.3% the samples are p-conductive, at 0.3% they show a high-ohmic behavior which gives a clear hint of an effective compensation mechanism. Figure 2a shows Raman spectra of the samples with lowest and highest Mg-

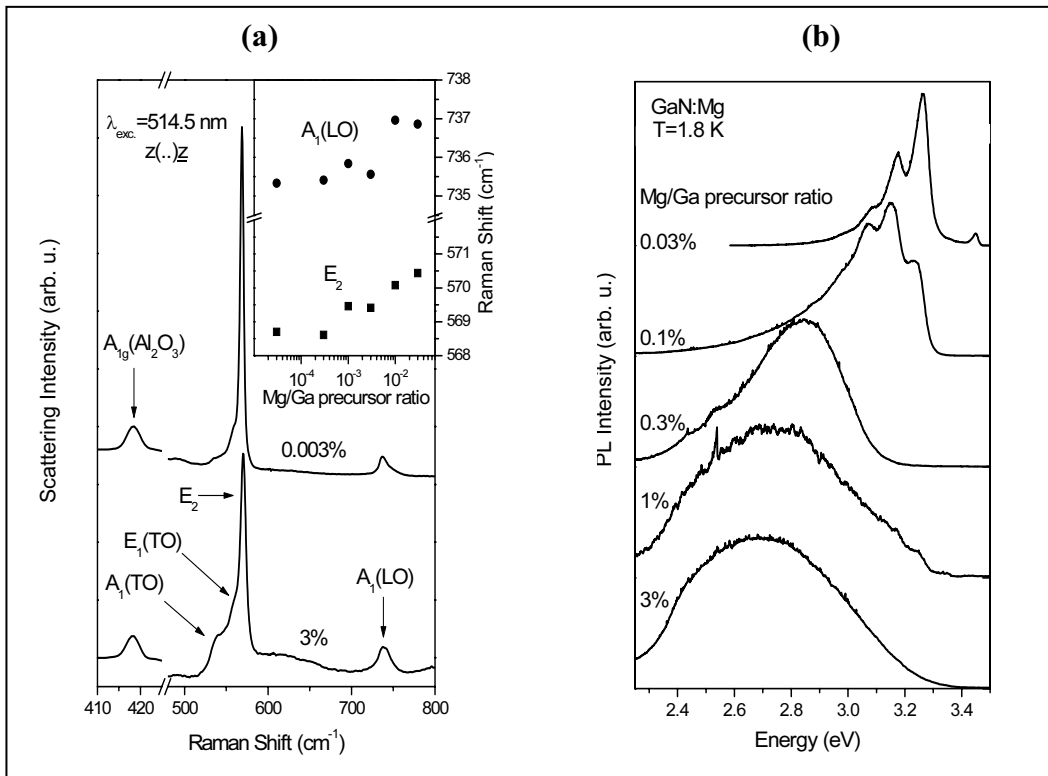


Fig. 2 a) Raman spectra of two GaN:Mg samples having different Mg content. Inset: Line position of the A₁(LO)- and the E₂-mode as a function of the Mg concentration. b) Photoluminescence spectra of GaN epilayers as a function of the Mg content at 1.8 K.

concentrations. A strong increase of full widths at half maximum (FWHM) of the E_2 -mode from 3.7 to 7.0 cm^{-1} is seen. Additionally, an increase of the intensity of the $E_1(\text{TO})$ mode in the forbidden configuration $z(\cdot)\bar{z}$ is observable. The line broadening and the breakdown of the selection rules indicates that the crystal quality decreases as a function of Mg content through the incorporation of defects. Additionally, the E_2 -mode shifts to higher energies which indicates an increase of the compressive strain through the Mg incorporation.

The luminescence spectra in p-conductive GaN is dominated by the donor–acceptor pair (DAP) lines which have typical phonon replicas of the zero-phonon line at 3.27 eV (Fig. 2b). In higher doped samples, only a broad luminescence band appears. The maximum of this band is shifted to lower energies. This behavior is well known from high compensated ZnSe:N [3] and GaAs:Li [5].

For ZnSe:N the intensity behavior of the DAP can be explained in a dynamical model proposed by Shklovskii and Efros [6]. It involves strong fluctuations of the band gap at different positions in the sample caused by electric fields of a high number of compensated and thus, ionized donors and acceptors which are randomly distributed in the sample. At low excitation densities radiative DAP recombination takes place between the energetically lowest neutral donors and acceptors since photo-excited carriers relax quickly to these levels. At high excitation densities, the concentration of photo-excited carriers is high enough to neutralize most donors and acceptors and the band fluctuation should vanish. Thus, at the highest densities the well known structured DAP emission line shape as seen for samples with low compensation should be observed.

To test this model for GaN:Mg we studied the intensity dependence of the PL of the most resistive sample grown with a Mg/Ga precursor ratio of 0.3%. It is shown in Fig. 3 for different excitation conditions. Starting from lowest excitation intensities (left spectra) we observe two broad emission bands around 2.45 eV und 2.8 eV . Assuming a Gaussian line shape for both luminescence bands we fitted the spectra and obtained a very good agreement with the experiments. Raising the excitation density the

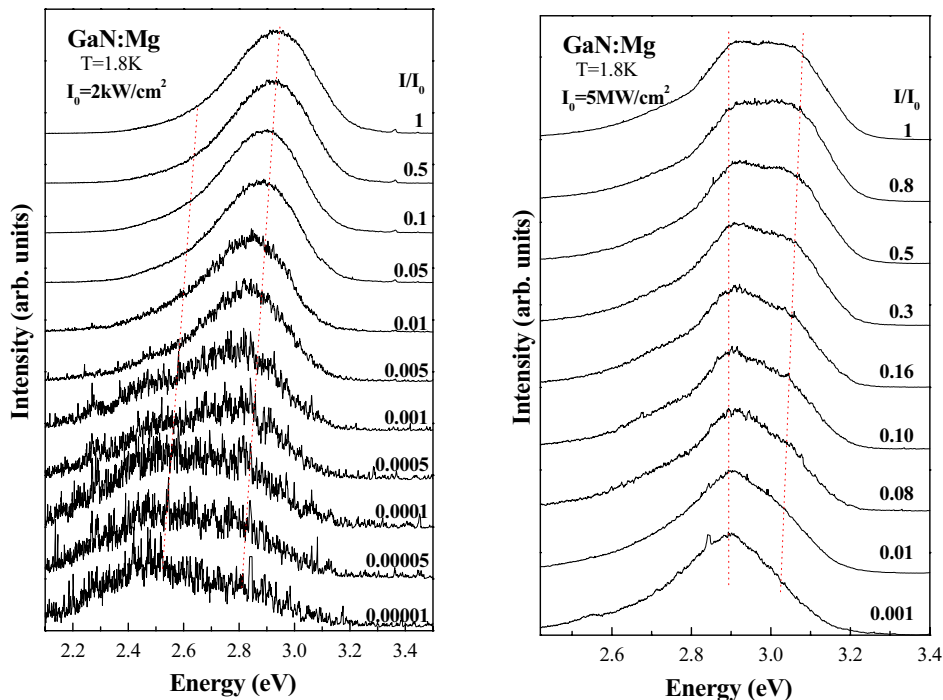


Fig. 3 (online colour at: www.interscience.wiley.com) Intensity dependence of normalized PL spectra in p-type GaN epilayers doped with 0.3% Mg (left part) measured with a cw HeCd laser up to 2 kW/cm^2 and (right part) with the third harmonic of a pulsed Nd:YAG laser with pulse intensities up to 5 MW/cm^2 .

high-energy band exhibits a growth in integrated intensity with a slope of unity, exactly the same as that observed in ZnSe:N. Also the observed logarithmic shift of the peak energy to higher energies with increasing excitation energies is in agreement with other strongly doped and compensated semiconductors. This shift is equal for both emission bands. The total blueshift of the high-energy luminescence between 20 mW/cm^2 and 2 kW/cm^2 amounts 153 meV. We find that the blueshift saturates at 2.91 eV. On the high-energy shoulder of this luminescence a new emission line grows, again shifting to higher energies with increasing intensity. At 5 MW/cm^2 the intensity maximum of this band is found at 3.06 eV, 210 meV below the zero phonon line of the DAP in weakly compensated GaN. Even, at highest excitation densities, no structured DAP band with typical LO-phonon replica was observed. The model of band fluctuations [6] cannot give a satisfying explanation for the behavior in highly compensated GaN:Mg. Therefore, we will now discuss a static model to explain the behavior of the DAP as a function of the excitation density. Certainly, static potential fluctuations here are not responsible for the observed effects but impurity bands of donors. From the energy positions of the saturated luminescence bands at 2.45 eV, 2.91 eV and 3.06 eV we could determine the corresponding donor levels considering the band gap of GaN and the acceptor energy. These levels lie 240 ± 30 , 350 ± 30 and 850 ± 30 meV below the conduction band [7, 8]. In the beginning all donors and acceptors are ionized. At low excitation densities a small number of donors and acceptors will be neutralized. The created electrons relax very fast in the deepest donor states. With increasing excitation density the donors will be neutralized one after another from the deepest to the highest energy state. This explains the observed blueshift with increasing excitation intensity. An additional blueshift takes place through the coulomb term between the ionized donors and acceptors. The energies of the deepest donor states are in very good agreement with values of 265 ± 15 meV, ca. 400 meV and 615 ± 20 meV in GaN:Mg determined by Hacke et al. [9] in DLTS investigations.

The shift of the „blue“ luminescence between 2.9 eV and 3.1 eV in hydrostatic pressure experiments with 20 meV/GPa is smaller than the shift of the DAP at 3.27 eV (33 meV/GPa) [10]. This is in contradiction to models which take into account shallow donor levels as initial states for this luminescence [11, 12] and supports the above explained model under consideration of deeper localized donor states.

3 Compensation of hydrogen and localized Mg–H vibrations in GaN:Mg (MOCVD)

During the MOCVD growth process of nitrides hydrogen is often present in the growth atmosphere in form of the carrier gases H_2 and NH_3 , respectively, or is bound in the organic precursor-molecules. During the dissociation process of these molecules at the surface hydrogen can be incorporated in the crystal. J. Neugebauer and C. G. Van de Walle [13] found in their calculation of the formation energies that under p-type conditions the incorporation of hydrogen is extremely efficient, while for n-GaN the mobility of hydrogen is very slow and so the hydrogen content is very low. This correlation could be found experimentally by Götz et al. [15]. The concentration of hydrogen is in the same range as the Mg-concentration [16]. Since hydrogen forms a shallow donor in GaN, often the as grown GaN epilayers are highly compensated and an activation of the acceptors is necessary.

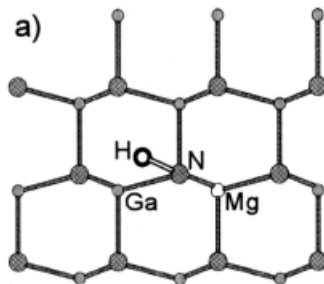


Fig. 4 Structure of the $\text{Mg}_{\text{Ga}}\text{-N-H}$ -complex after [14].

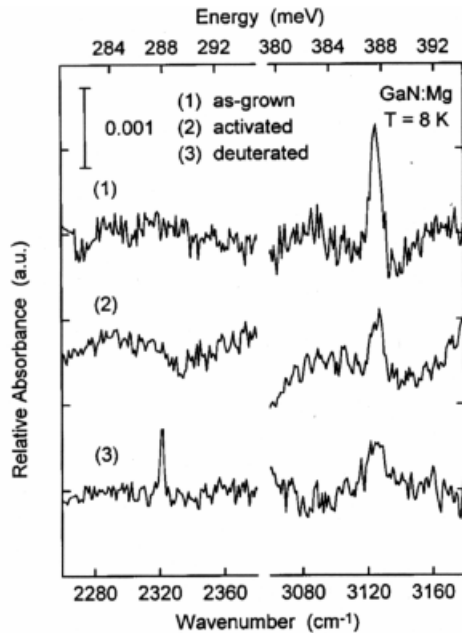


Fig. 5 IR-absorption spectra of GaN:Mg (MOCVD): (1) as-grown, (2) after thermal annealing, and (3) after deuteration [17].

The electrical compensation takes place by the formation of a Mg–H-complex, the corresponding atomic structure (seen in Fig. 4) was proposed by [13] as a $\text{Mg}_{\text{Ga}}\text{-N-H}$ -complex. The exceptional feature is that no direct Mg–H-bonds can be achieved. On the basis of a large ionicity of the Ga–N-bond the hydrogen atom prefers to incorporate on an antibonding site of the nitrogen. The vibronic frequency of the complex is mainly determined by the N–H vibrational mode. The predicted value is 3360 cm^{-1} , nearby the frequency of the NH_3 stretch mode with 3444 cm^{-1} .

In infrared absorption spectra of GaN:Mg (MOCVD) a localized vibrational mode (LVM) was found at 3125 cm^{-1} [17, 18]. After activation of compensated GaN samples through thermal annealing p-conductance and a simultaneously strong decrease of the intensity of the LVM could be observed. Through deuteration a second absorption line having a frequency of 2321 cm^{-1} could be generated (Fig. 5). The frequency ratio between both LVMs is $1.346 \approx \sqrt{2}$. This value would be expected if one take into account a mass change during an isotope substitution from hydrogen through deuterium. This is a strong experimental evidence that the mode at 3125 cm^{-1} can be attributed to a defect complex of $\text{Mg}_{\text{Ga}}\text{-N-H}$.

4 Mg-doped GaN grown by molecular beam epitaxy – high energy Raman modes

In contrary to GaN:Mg grown by MOCVD the Mg doped MBE samples show p-conductivity in the as grown state [19]. This could be put down to the fact that the MBE chamber has ultrahigh vacuum conditions and so no compensating hydrogen can be incorporated during the growth procedure. One has to take into account that the remaining vapor pressure in the MBE chamber mainly consists of H_2 . In addition to that it could be shown by mass spectroscopy that the Mg sources often release hydrogen during the evaporation process [20].

Raman spectra of Mg-doped GaN grown by MBE show at high energies LVMs having at 4 K the following frequencies: $2129, 2148, 2166, 2185, 2204$ und 2219 cm^{-1} [21, 22]. Four of these modes ($2151, 2168, 2185, 2219\text{ cm}^{-1}$) has been observed earlier by Brandt et al. [20]. In Fig. 6a the correlation between the Mg concentration and the appearance of the high-energy modes is seen. At doping levels of $8 \times 10^{19}\text{ cm}^{-3}$ a fine structure between 2129 and 2219 cm^{-1} occurs. Reducing the Mg concentration to $6 \times 10^{18}\text{ cm}^{-3}$ in the chosen spectral range only the stretch vibration of N_2 (2329 cm^{-1} [23]) is seen while the other Raman-active modes are not observable. For concentrations in between the new modes start to grow up.

The high energy defect modes show a distinct A_1 -symmetry (Fig. 6b). Only, the modes at 2166 and 2219 cm^{-1} are seen in crossed polarization having a weak intensity in the spectra. However, only these both modes are infrared active [20]. As a result, two different groups of defect complexes can be distinguished, however, the dipole moment of the infrared active mode cannot be parallel to the c -axis. The dipole moment of the other vibrational modes does not change or is oriented parallel to the c -axis.

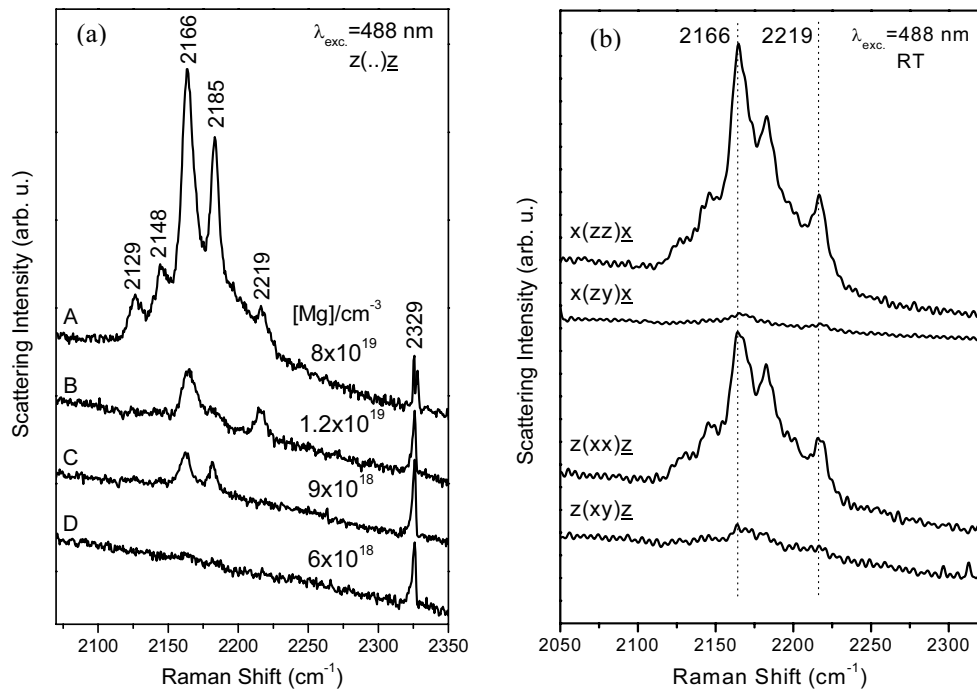


Fig. 6 a) RT Raman spectra of GaN:Mg (MBE) in the high-energy range around 2200 cm^{-1} as a function of the Mg content. b) Polarization dependence of the high-energy modes in GaN:Mg.

The vibrational frequencies of more than 2200 cm^{-1} are typical for defects including hydrogen as complex partner. Similar complexes are wellknown in other semiconductor materials, as i.e. ZnSe:As,H with a frequency of 2165 cm^{-1} or in GaAs:C,H at 2628 cm^{-1} [25]. Similar high-energy vibrations could be expected for N- (see N_2 -stretch vibration at 2329 cm^{-1}) or for C with a threefold binding. Nevertheless, it was not clear for a long time, if really the responsible complex for the observed Raman modes includes hydrogen. First of all, the modes were only found in MBE grown material, even though the growth atmosphere includes much less hydrogen compared to the MOCVD growth, if not NH_3 was used as nitrogen source. In the beginning of this chapter was described how hydrogen can contaminate the samples during the MBE growth. Secondly, the predicted $\text{Mg}_{\text{Ga}}\text{-N-H}$ complex could be detected and so no other obvious explanation of a complex in the energy range around 2200 cm^{-1} is possible.

Investigations of Harima et al. [24, 26] could clearly show the correlation of the hydrogen incorporation during their different growth conditions. Through thermal annealing of GaN:Mg (MOCVD) above 600°C the $\text{Mg}_{\text{Ga}}\text{-N-H}$ complex will be destroyed. Simultaneously, the before compensated material will be p-conductive. For temperatures above 700°C the above mentioned defect modes around 2200 cm^{-1} from the MBE material occur (Fig. 7). If during the MOCVD growth process N_2 was used as carrier gas instead of H_2 , neither before nor after thermal annealing the high-energy vibrational modes could be found. These results give a clear evidence for the following interpretation. During the thermal annealing procedure a reorientation of the initial $\text{Mg}_{\text{Ga}}\text{-N-H}$ complex takes place compensating the Mg acceptor through hydrogen. New complexes were formed which were found in GaN:Mg grown by MBE. These defect complexes includes as well hydrogen, however, here the hydrogen is electrical inactive and is not compensating in this configuration. In conclusion we have now an efficient tool to determine the degree of compensation and the p-conductivity with the above mentioned Raman spectroscopy, if one detect the high-energy modes in GaN: Mg.

If one anneal p-type GaN samples grown by MBE in a N_2 or N_2+NH_3 atmosphere [21], it is not possible to increase the p-conductance. The epilayers show at annealing temperatures of 930°C rather a high-ohmic behavior, while a change of the relative intensities of the different local defect modes is observed

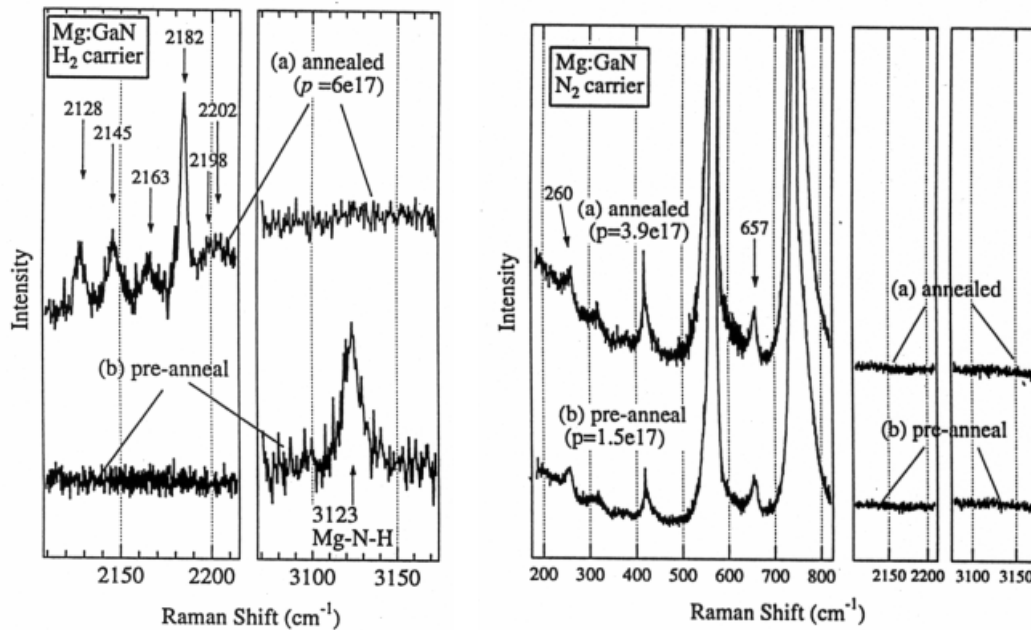
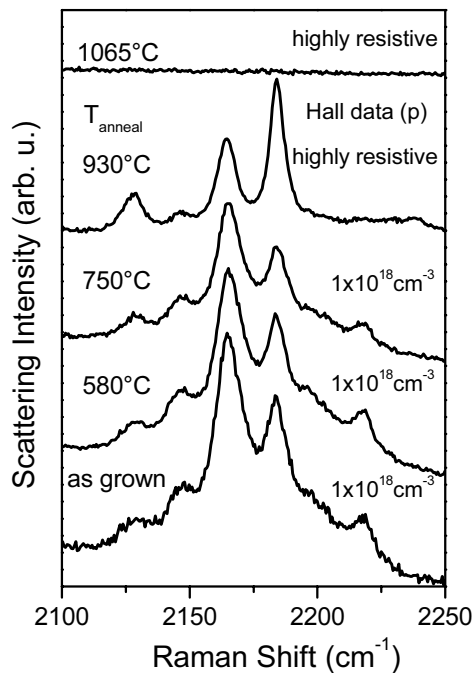


Fig. 7 Raman spectra of GaN:Mg (MOCVD) using H₂ (left part) and N₂ (right part) as transport gas before (b) and after annealing (a) [24].

simultaneously (Fig. 8). At temperatures of 1065 °C, which are typical for the MOCVD growth, all defect modes disappear and the samples are highly compensated. Now, no reorientation to the Mg_{Ga}-N-H complex takes place. The worsen conductance can be attributed to the generation of new defects at higher temperatures. A drastic change of the sample quality can be prevented by the N₂ partial pressure during the annealing procedure. Since the Mg-correlated vibrational modes disappeared totally, an out-diffusion or reorientation of the Mg atoms is more probable.



The distinct atomic structure of the defect complexes is not understood totally. A comparison with other materials [27] suggests Ga-H- (2171 cm⁻¹ in Si) and Mg-H-defects (2144 cm⁻¹ in GaAs) as possible candidates. However, V_{Ga}-H_N-defect complexes [28] are relatively improbable (3000–3100 cm⁻¹ in GaN). To explain the multitude of vibrational modes there are different models which have to be considered.

Fig. 8 Raman spectra of the high energy LVMS after annealing at different temperatures

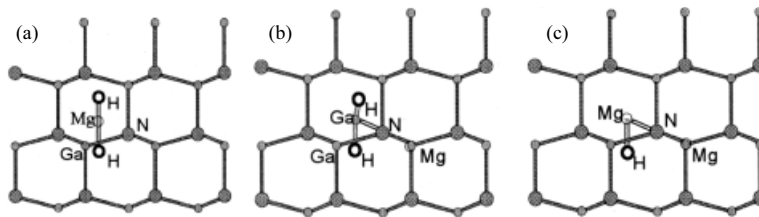
Table 1 Comparison of the relative intensities of the high-energy modes in GaN:Mg with the natural abundance of the three Mg isotopes.

Mg-isotope	nat. abundance	$\omega_{\text{theor.}} (\text{cm}^{-1})$	$\omega_{\text{GaN:Mg}} (\text{cm}^{-1})$	rel. intensity
26	11%	2129 / 2148	2129 / 2148	3% / 10%
25	10%	2171 / 2190	2166 / 2185	40% / 24%
24	79%	2215 / 2235	2204 / 2219	10% / 13%

1. The number of six modes could be understood through an isotope effect. The Mg used in the Knudsen-cells of the MBE has the natural abundance of isotopes. Native Mg has stable isotopes with mass numbers 24, 25 and 26 and with an abundance of 79%, 10% and 11%. If one take into account that the modes at 2129 and 2148 cm^{-1} originate from defects with the isotope mass number of 26, then we receive as vibrational frequencies of the same complex with ^{25}Mg (^{24}Mg) 2171 (2215) and 2190 cm^{-1} (2235 cm^{-1}). To explain the experimental results with an isotope effect

the relative intensities of the Raman modes must correspond to the natural abundance of isotopes. This correlation was not observed (see Table 1). Furthermore, in this model it is impossible to understand the special behavior of the local modes at 2168 and 2219 cm^{-1} .

2. The p-doping is a complex process where Mg does not only be incorporated on lattice places. It is very probable that substitutional and interstitial (SI) defect complexes participating by Mg can be created. Reboredo and Pantelides [14] calculated *ab initio* the vibrational frequencies of such defect structures. They proposed SI complexes schematically shown in Fig. 9 with Mg- and Ga-atoms on interstitial sites where hydrogen atoms of different binding length are bound. Since the $\text{Ga}_i\text{-H}$ -bonds are not exactly orientated parallel to the c -axis, it is possible that the defect complex $\text{Mg}_{\text{Ga}^-}\text{-N-Ga-H}_2$ is responsible for the IR-active modes at 2166 und 2219 cm^{-1} . As seen in Table 2 the presented comparison between experimental and theoretical values are relatively large. An uncertainty of 200 cm^{-1} through the theoretical method is without any additional parameter quite legitimately. For deviations larger than 500 cm^{-1} , the prediction is not acceptable. The authors put forward anharmonic effects for this large deviations. The prediction that the postulated SI-H-defects are reorientated through thermal annealing mechanisms to $\text{Mg}_{\text{Ga}^-}\text{-N-H}$ -complexes could not be confirmed. Furthermore, our investigations in this paper and the results of Harima et al. [24, 26] differ from the predictions of Reboredo et al. [14].

**Fig. 9** Postulated Mg-H complexes in GaN [14]: a) Mg_iH_2 , b) $\text{Mg}_{\text{Ga}^-}\text{-N-Ga-H}_2$, and c) $\text{Mg}_{\text{Ga}^-}\text{-N-Mg}_i\text{-H}$.**Table 2** Comparison of calculated vibrational frequencies of different H-correlated defect complexes with experimental values.

defect complex lt. [14]	$\omega_{\text{theor.}} (\text{cm}^{-1})$	$\omega_{\text{GaN:Mg}} (\text{cm}^{-1})$
Mg_iH_2 (short bond)	2001	2185
Mg_iH_2 (long bond)	1570	2148
$\text{Mg}_{\text{Ga}^-}\text{-N-Ga-H}_2$ (short bond)	2270	2219
$\text{Mg}_{\text{Ga}^-}\text{-N-Ga-H}_2$ (long bond)	1500	2166
$\text{Mg}_{\text{Ga}^-}\text{-N-Mg}_i\text{-H}$	1320	–

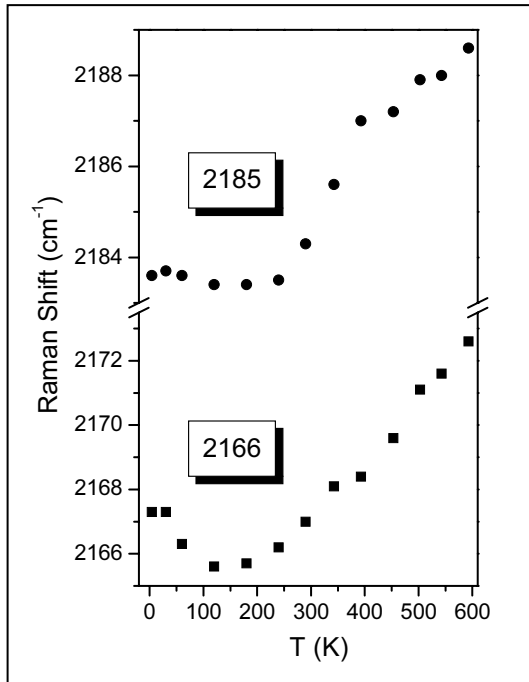


Fig. 10 Raman shift of the two prominent high-energy modes in GaN:Mg as a function of the lattice temperature.

With the discussed interpretations it is not possible to attribute free of doubts the observed Raman modes. Most probable is the attribution to defect complexes which contains as well magnesium and hydrogen as intrinsic defects, like vacancies, atoms on interstitials or dislocations. A possible proof of the correct attribution to the theoretically postulated defects is given by the temperature dependence of the high-energy modes. In Fig. 10 a line shift to higher energies with increasing temperatures is clearly visible. This is remarkable, since through the thermal expansion of the lattice a shift to lower energies should take place [29]. The E_2 mode of the host lattice shifts in the temperature range between 4 K and 590 K around 6 cm^{-1} to lower energies, while the energies of the

defect modes shift in the same temperature range around 5 cm^{-1} to higher energies. This different temperature dependent behavior of LVMs compared to the host lattice phonons is typical, here the negative lattice expansion coefficient at low temperatures plays an important role for the binding process at the impurity hydrogen complex.

5 Low-energy modes in Raman investigations

Simultaneously with the appearance of the high-energy modes five local vibrational modes in addition to host modes can be observed in the range of the acoustical and optical phonons in GaN:Mg. The phonon energies at room temperature are $136, 262, 320, 595$ and 656 cm^{-1} . The intensity of these modes scales as well with Mg content in the sample. All modes have A_1 -symmetry (Fig. 11). Both structures with large FWHM at 320 and 595 cm^{-1} can be attributed to scattering processes of phonons beyond the Γ -point through a comparison with the phonon density of states (Fig. 12). Through the incorporation of defects the momentum conservation of the Raman process weakens and therefore also the reduction of the observable phonons around $q = 0$. For strongly perturbed crystals the phonon density of states folded with the phonon occupation can be observed in first order Raman spectra. This interpretation is supported through the fact that with increasing Mg concentration the intensity of $A_1(\text{TO})$ -mode in the forbidden $z(\cdot)\bar{z}$ configuration increases. The energy position of 320 cm^{-1} is in good agreement with the observed disorder Raman mode at 300 cm^{-1} which is activated by ion implantation in GaN [30]. The modes at $136, 262$ and 656 cm^{-1} cannot be put down to disorder activated scattering processes, since the phonon dispersion curve in this range have no large density of states. The authors of Ref. [31] report on a mode at 656 cm^{-1} which occurs in GaN/sapphire after thermal annealing at $1000 \text{ }^\circ\text{C}$. Lattice vibrations of disordered sapphire was given as explanation. In contrary the mode we found at the same energy position does not scale with the A_{1g} -mode of sapphire at 418 cm^{-1} or with the mode of disordered sapphire at 770 cm^{-1} , but with the Mg content. An interpretation of these vibrations as LVMs of Mg can easily be understood. An estimation of LVM frequencies can be done by the effective masses of Ga-N- und Mg-

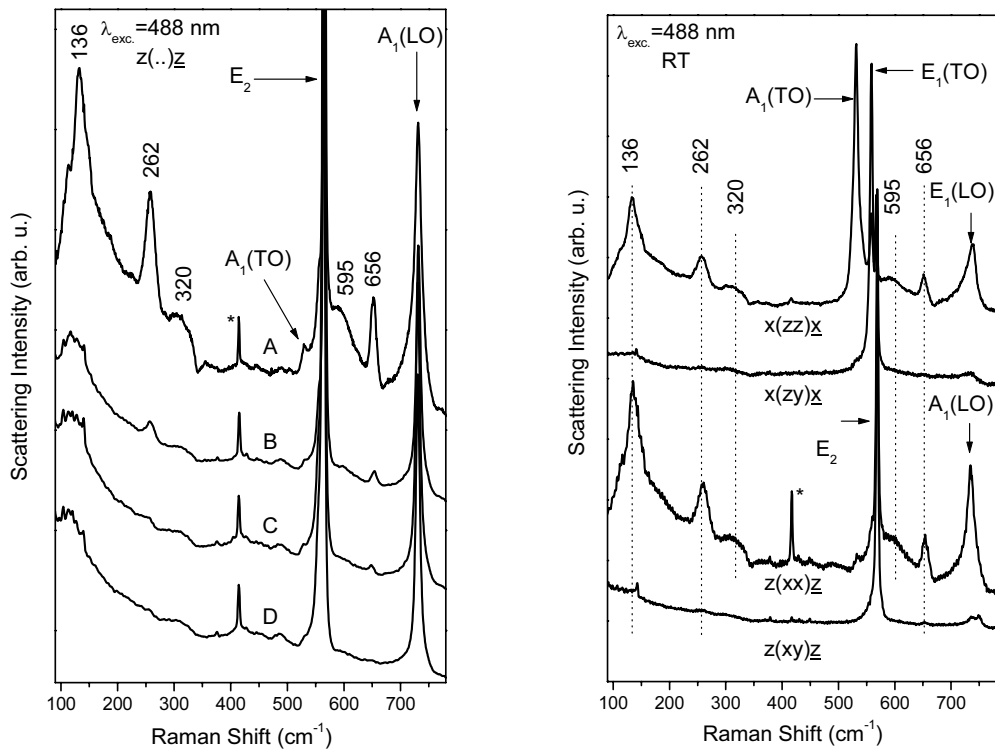


Fig. 11 Normalized Raman spectra in the range of the host phonons of GaN for various Mg doping (left part). The polarization dependence of the low-energy modes is shown in the right figure. The A_{1g}-mode of the sapphire substrate is marked by an asterisk.

N-vibrations.

$$\frac{\omega_{\text{GaN}}}{\omega_{\text{LVM}}} = \sqrt{\frac{\mu_{\text{LVM}}}{\mu_{\text{GaN}}}} \quad (1)$$

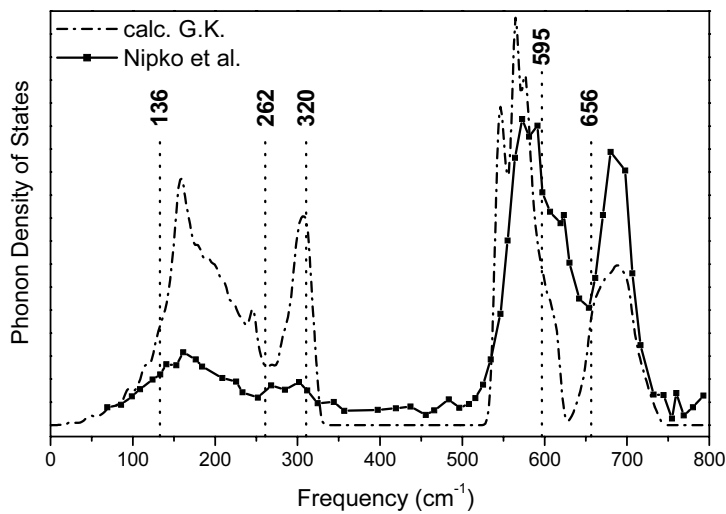


Fig. 12 Comparison of experimental determined PDOS of GaN from neutron scattering investigations [32] and a PDOS calculated by a valence force model [33]. The dashed lines mark the position of the low-energy modes in GaN:Mg.

If one take into account that Mg is incorporated on a Ga lattice site and put in $\omega_{GaN} = \omega[E_1(TO)] = 560 \text{ cm}^{-1}$, a value of 640 cm^{-1} for Mg–N-vibration can be determined, which is in good agreement with the experimentally found value of 656 cm^{-1} . Calculating the LVMs of Mg_{Ga} in a valence force model of Kane we received frequencies of $132, 267$ und 660 cm^{-1} with a scaling factor of -0.15 [33]. This means that the binding forces in the neighborhood of Mg_{Ga} is around 15% smaller in comparison to the host crystal, which is in agreement with values in other semiconductor materials [34]. The explanation of low-energy modes as LVM of Mg was confirmed by H. Harima et al. [26]. Furthermore, a direct correlation between the hole concentration and the intensity of the LVMs could be found. This shows that the intensities of the modes are a direct measure for the concentration of activated Mg.

6 Conclusion

In GaN:Mg two main compensation mechanisms of Mg acceptors occur. One mechanism is the self-compensation effect. The incorporation of Mg causes a local perturbation of the crystal structure which creates defects acting as donors and compensating acceptors. Through intensity dependent PL-investigations a DAP model for high compensating GaN:Mg could be found and the energy position of compensating donor states could be determined.

In particular for GaN epilayers grown by MOCVD compensation mechanisms with hydrogen play an important role besides the self-compensation effects. Such Mg-doped samples show as grown high-ohmic behavior and an annealing procedure is necessary to activate the acceptors. In MOCVD samples a vibrational mode at 3125 cm^{-1} could be attributed to the $\text{Mg}_{Ga}\text{-N-H}$ defect complex.

Mg-doped MBE samples are p-conductive without any further post growth treatment. Those samples show in Raman spectra a series of LVMs in the range around 2200 cm^{-1} and in the range of the host modes. The high-energy modes originate from defect complexes which are created through a thermal annealing procedure from the $\text{Mg}_{Ga}\text{-N-H}$ -complex. A clear correlation with the incorporation of hydrogen exists. The low-energy modes consist of two groups. The modes at 320 and 595 cm^{-1} are activated through disorder and reflect a range of the phonon density of states. The Raman modes at $136, 262$ and 656 cm^{-1} can be attributed to LVMs of Mg. The high- as well as the low-energy modes only appear in p-conductive GaN:Mg. Investigating the intensity dependence of the different Mg–H-complexes and the LVM of activated Mg the Raman spectra give a clear direct evidence of the degree of compensation and p-conductivity.

References

- [1] H. Amano, M. Kito, K. Hiramatsu, and I. Akasaki, *Jpn. J. Appl. Phys., Part 2*, **28**, L2112 (1989).
- [2] S. Nakamura, N. Iwasa, M. Senoh, and T. Mukai, *Jpn. J. Appl. Phys., Part 1*, **31**, 1258 (1992).
- [3] R. Heitz, E. Moll, V. Kutzer, D. Wiesmann, B. Lummer, A. Hoffmann, I. Broser, P. Bäume, W. Taudt, J. Söllner, and M. Heuken, *J. Cryst. Growth* **159**, 307 (1996).
- [4] U. Kaufmann, P. Schlotter, H. Obloh, K. Köhler, and M. Maier, *Phys. Rev. B* **62**, 10867 (2000).
- [5] H. P. Gislason, B. H. Yang, and M. Linnarson, *Phys. Rev. B* **47**, 9418 (1993).
- [6] B. I. Shklovskii and A. L. Efros, *Electronic Properties of Doped Semiconductors*, (Springer-Verlag, Berlin, Heidelberg, New York, 1984), pp. 52.
- [7] L. Eckey, *Exzitonen im Galliumnitrid- Struktur und Dynamik*, Dissertation, TU Berlin, 1998.
- [8] L. Eckey, U. von Gfug, J. Holst, A. Hoffmann, A. Kaschner, H. Siegle, C. Thomsen, B. Schineller, K. Heime, M. Heuken, O. Schön, and R. Beccard, *J. Appl. Phys.* **84**, 5828 (1998).
- [9] P. Hacke, H. Nakayama, T. Detchprohm, K. Hiramatsu, and N. Sawaki, *Appl. Phys. Lett.* **68**, 1362 (1996).
- [10] H. Teisseyre, T. Suski, P. Perlin, I. Grzegory, M. Leszczynski, M. Bockowski, S. Porowski, J. A. Freitas, Jr., R. L. Henry, A. E. Wickeden, and D. D. Koleske, *Phys. Rev. B* **62**, 10151 (2000).
- [11] M. Smith, G. D. Chen, H. X. Jiang, A. Salvador, B. N. Sverdlov, A. Botchkarev, H. Morkoç, and B. Goldenberg, *Appl. Phys. Lett.* **68**, 1883 (1996).
- [12] E. Oh, H. Park, and Y. Park, *Appl. Phys. Lett.* **72**, 70 (1998).
- [13] J. Neugebauer and C. G. Van de Walle, *Phys. Rev. Lett.* **75**, 4452 (1995).

- [14] F. A. Reboredo and S. T. Pantelides, *Phys. Rev. Lett.* **82**, 1887 (1999).
- [15] W. Götz, N. M. Johnson, J. Walker, D. P. Bour, H. Amano, and I. Akasaki, *Appl. Phys. Lett.* **67**, 2666 (1995).
- [16] L. Sugiura, M. Suzuki, and J. Nishio, *Appl. Phys. Lett.* **72**, 1748 (1998).
- [17] W. Götz, N. M. Johnson, D. P. Bour, M. D. McCluskey, and E. E. Haller, *Appl. Phys. Lett.* **69**, 3725 (1996).
- [18] B. Clerjaud, D. Côte, A. Lebkiri, C. Naud, J. M. Baranowski, K. Pakula, D. Wasik, T. Suski, *Phys. Rev. B* **61**, 8238 (2000).
- [19] T. D. Moustakas and R. Molnar, *Mater. Res. Soc. Symp. Proc.* **281**, 753 (1993).
- [20] M. S. Brandt, J. W. Ager III, W. Götz, N. M. Johnson, J. S. Harris, Jr., R. J. Molnar, and T. D. Moustakas, *Phys. Rev. B* **49**, 14758 (1994).
- [21] A. Kaschner, G. Kaczmarczyk, A. Hoffmann, C. Thomsen, U. Birkle, S. Einfeldt, and D. Hommel, *phys. stat. sol. (b)* **216**, 551 (1999).
- [22] A. Kaschner, *Lokalisierung, Defekte und Verspannung in Gruppe-III Nitriden*, Dissertation, TU Berlin, 2001.
- [23] F. Rasetti, *Phys. Rev.* **34**, 367 (1929).
- [24] H. Harima, T. Inoue, Y. Sone, S. Nakashima, M. Ishida, and M. Taneya, *phys. stat. sol. (b)* **216**, 789 (1999).
- [25] M. D. McCluskey and N. M. Johnson, *J. Vac. Sci. Technol. A* **17**, 2188 (1999).
- [26] H. Harima, T. Inoue, S. Nakashima, M. Ishida, and M. Taneya, *Appl. Phys. Lett.* **75**, 1383 (1999).
- [27] S. J. Pearton, J. W. Corbett, and M. Stavola, *Hydrogen in Crystalline Semiconductors*, (Springer-Verlag, Berlin/Heidelberg/New York, 1991), and references therein.
- [28] M. G. Weinstein, C. Y. Yong, M. Stavola, S. J. Pearton, R. J. Wilson, R. J. Shul, K. P. Kileen, and M. J. Ludowise, *Appl. Phys. Lett.* **72**, 2589 (1998).
- [29] W. S. Li, Z. X. Shen, Z. C. Feng, and S. J. Chua, *J. Appl. Phys.* **87**, 3332 (2000).
- [30] W. Limmer, W. Ritter, R. Sauer, B. Mensching, C. Liu, and B. Rauschenbach, *Appl. Phys. Lett.* **72**, 2589 (1998).
- [31] M. Kuball, F. Demangeot, J. Frandon, M. A. Renucci, J. Massies, N. Grandjean, R. L. Aulombard, and O. Briot, *Appl. Phys. Lett.* **73**, 969 (1998).
- [32] J. C. Nipko, C.-K. Loong, C. M. Balkas, and R. F. Davis, *Appl. Phys. Lett.* **73**, 34 (1998).
- [33] A. Kaschner, A. Hoffmann, C. Thomsen, T. Böttcher, S. Einfeldt, and D. Hommel, *phys. stat. sol. (a)* **174**, R4 (2000).
- [34] R. C. Newman, E. G. Grosche, M. J. Ashwin, B. R. Davidson, D. A. Robbie, R. S. Leigh, and M. J. L. Sangster, *Mater. Sci. Forum* **258-263**, 1 (1997).